ACS Catalysis

pubs.acs.org/acscatalysis

Research Article

General Pyrrolidine Synthesis via Iridium-Catalyzed Reductive Azomethine Ylide Generation from Tertiary Amides and Lactams

Ken Yamazaki,[§] Pablo Gabriel,[§] Graziano Di Carmine, Julia Pedroni, Mirxan Farizyan, Trevor A. Hamlin,* and Darren J. Dixon*

Cite This: *ACS Catal.* 2021, 11, 7489–7497

Read Online

ACCESS | Metrics & More | Article Recommendations | Supporting Information

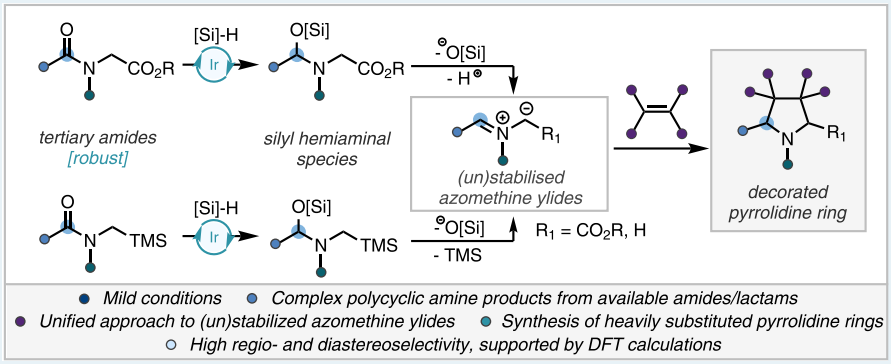

ABSTRACT: An iridium-catalyzed reductive generation of both stabilized and unstabilized azomethine ylides and their application to functionalized pyrrolidine synthesis via [3 + 2] dipolar cycloaddition reactions is described. Proceeding under mild reaction conditions from both amide and lactam precursors possessing a suitably positioned electron-withdrawing or a trimethylsilyl group, using 1 mol% Vaska's complex [$IrCl(CO)(PPh_3)_2$] and tetramethyldisiloxane (TMDS) as a terminal reductant, a broad range of (un)stabilized azomethine ylides were accessible. Subsequent regio- and diastereoselective, inter- and intramolecular dipolar cycloaddition reactions with variously substituted electron-deficient alkenes enabled ready and efficient access to structurally complex pyrrolidine architectures. Density functional theory (DFT) calculations of the dipolar cycloaddition reactions uncovered an intimate balance between asynchronicity and interaction energies of transition structures, which ultimately control the unusual selectivities observed in certain cases.

KEYWORDS: *Vaska's complex, amide reduction, [3 + 2] cycloaddition, azomethine ylide, pyrrolidines, polycyclic amine, density functional calculations*

INTRODUCTION

Saturated pyrrolidine heterocycles are prevalent in biologically active natural products and are among the 10 most common ring systems in small drug molecules (Scheme 1A).[1−4] Accordingly, new broad scope methods for their synthesis remain important. While relatively simple pyrrolidine derivatives are commercially available, polysubstituted pyrrolidines generally require synthetic effort. To this end, [3 + 2] dipolar cycloadditions of azomethine ylides are synthetically powerful, allowing the direct construction of the saturated five-membered ring system with control over up to four newly formed stereogenic centers in an atom-economic reaction.[5] Consequently, the synthesis and reactions of azomethine ylides have been the focus of a number of research efforts over the years (Scheme 1B). These dipoles can be prepared from the opening of an aziridine ring[6i] or more commonly from the activation of an imine/iminium ion species (usually accessed from the condensation of an aldehyde and a primary or secondary amine either *in* or *ex situ*) and are especially useful for the synthesis of pyrrolidines unsubstituted on the nitrogen atom.[5c,6s] Other methods also exist, requiring the construction of finely tuned precursors.[6aa] Notwithstanding these many advances, to date, a general reductive strategy for azomethine ylide 1,3-dipole generation from tertiary amides and lactams enabling downstream access to desirable pyrrolidine structures remains unsolved.[6af] Toward this end and building on our program on reductive manipulation of amide functional groups,[7] we reasoned that iridium-catalyzed hydrosilylation of suitably functionalized tertiary amides and lactams could

Received: April 7, 2021
Revised: May 19, 2021
Published: June 9, 2021

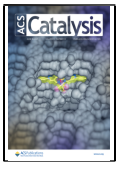

https://doi.org/10.1021/acscatal.1c01589
ACS Catal. 2021, 11, 7489–7497

Scheme 1. (A) Selected Examples of Natural Products and Drug Molecules Containing Decorated Pyrrolidine Rings. Ar = 4-OMeC$_6$H$_4$. (B) Traditional Synthetic Methods for the Preparation of Azomethine Ylides. (C) Iridium-Catalyzed Reductive Generation of (Un)stabilized Azomethine Ylides for 1,3-Dipolar Cycloaddition Reactions

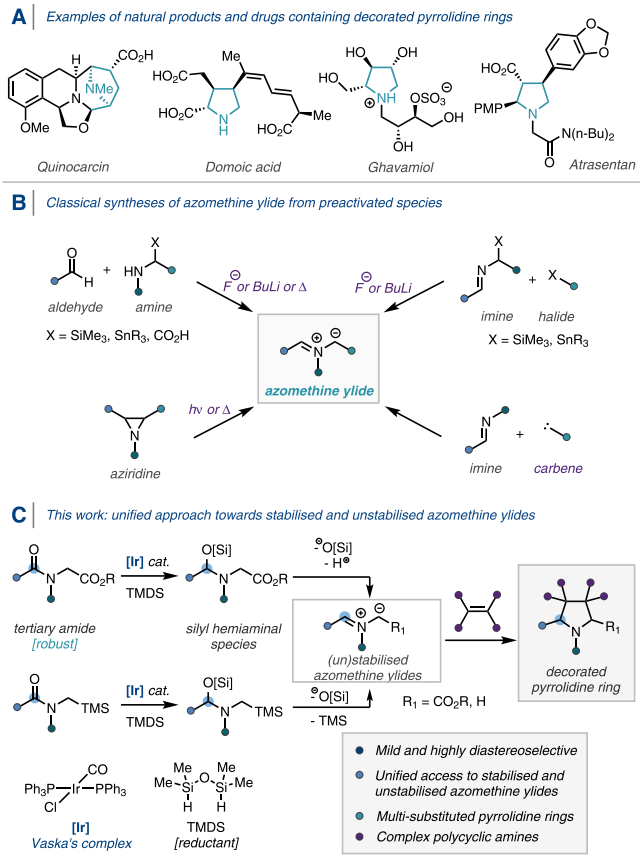

provide a new entry point. With substrates possessing a suitably positioned electron-withdrawing or a trimethylsilyl group, following partial reduction and subsequent silanoate elimination, concomitant deprotonation or loss of a trimethylsilyl group adjacent to the iminium ion could feasibly generate the synthetically versatile azomethine ylide (Scheme 1C). Subsequent cycloaddition reaction with dipolarophiles would then give access to the decorated pyrrolidine ring in a convenient one-pot process. Such a strategy would potentially provide an avenue for the late-stage synthesis of highly functionalized pyrrolidines from stable and widely abundant amides, under mild conditions, while eliminating the need for handling sensitive amine functionalities. Herein, we wish to describe our findings.

RESULTS AND DISCUSSION

Optimization Studies. Proline methyl ester benzoylamide derivative **1a** was chosen as a model system to investigate the transformation, alongside oxazolidinone dipolarophile **2a**, selected for its previous use in [3 + 2] cycloadditions and for its easy downstream derivatization.[8] Using 1 mol % IrCl(CO)(PPh$_3$)$_2$ (Vaska's complex) and 2 equiv of tetramethyldisiloxane (TMDS) for partial amide reduction, plus additional triethylamine as a Brønsted base for the generation of the dipole, we were pleased to isolate the desired product **3a** in a 50% yield as a single diastereoisomer,

Scheme 2. Iridium-Catalyzed Reductive Dipole Generation and Reaction Optimization Studies

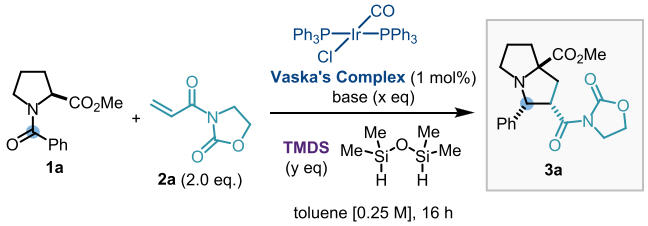

entry[a]	TMDS (y eq)	base (x eq)	temp. (°C)	3a (%)[b]
1	2.0	NEt_3 (2.0)	rt	50
2	2.0	-	rt	88 (86)
3	1.2	-	rt	65
4	2.0	-	80	74

[a]General conditions: **1a** (0.25 mmol scale), IrCl(CO)(PPh$_3$)$_2$ (1 mol %), additive, 1,1,3,3-tetramethyldisiloxane (TMDS), toluene (1 mL), rt, 16 h. [b]NMR yield calculated with 1,3,5-trimethoxybenzene as an internal standard; isolated yield in parentheses.

indicating the formation and subsequent stereoselective cycloaddition of the azomethine ylide (Scheme 2, entry 1). Notably, a control experiment revealed that no additional base was required for the reaction to proceed (entries 1 and 2), indicating that the eliminated silanoate was indeed a competent Brønsted base for dipole generation (see Scheme 1C). The use of 2 equiv of TMDS was optimal (entries 2 and 3), and the reaction could also proceed at higher temperature, albeit in a slightly reduced yield (entries 2 and 4). Therefore, entry 2 was chosen as standard conditions for assessing the scope of the reaction.

Scope Development. With the optimal reaction conditions in hand, we explored the scope of the [3 + 2] cycloaddition reaction with a range of electron-deficient alkenes as coupling partners. A 1,1′-disubstituted methacrylic acid derivative successfully underwent cyclization to give a cycloadduct possessing a quaternary carbon center (**3b**), while crotonic and cinnamic acid derivatives gave rise to the corresponding polysubstituted products bearing four adjacent stereocenters in good yields with high diastereoselectivity (**3c**, **3d**). Importantly, the reaction was not limited to *N*-enoyl oxazolidinone coupling partners; acrylate, furanone, nitroalkene, cinnamate, and vinyl sulfone derivatives (**3e**−**3i**, respectively) all produced the desired cycloadducts, with a large diversity of substitution patterns on the pyrrolidine ring, and in good to excellent yields. Interestingly, the regioselectivity of the formation of **3h** was reversed when compared to **3d**, as confirmed by single-crystal X-ray diffraction analysis, while **3g** and **3i** were formed as a 1:1 mixture of the two regioisomers (in line with the literature precedent) (Scheme 3).[9]

Pleasingly, the reaction sequence was found to be general with respect to the amide substrate. The presence of a methyl ester was found not to be a limiting requirement (**3j**, **3m**), while the azetidine-containing amino acid derivative afforded the corresponding [3,2,0] bicyclic compound in moderate yield (**3k**). Importantly, this methodology could also be applied to lactam substrates, providing bicyclic cycloadducts containing a tertiary stereocenter adjacent to the nitrogen atom, which would otherwise be inaccessible from other azomethine ylide generation methods (**3l**−**3n**).

https://doi.org/10.1021/acscatal.1c01589
ACS Catal. 2021, 11, 7489−7497

Scheme 3. Substrate Scope of the [3 + 2] Cycloaddition via Stabilized Azomethine Ylides with Regard to the Dipolarophile (A) and the Amide or Lactam Substrates (B)[a]

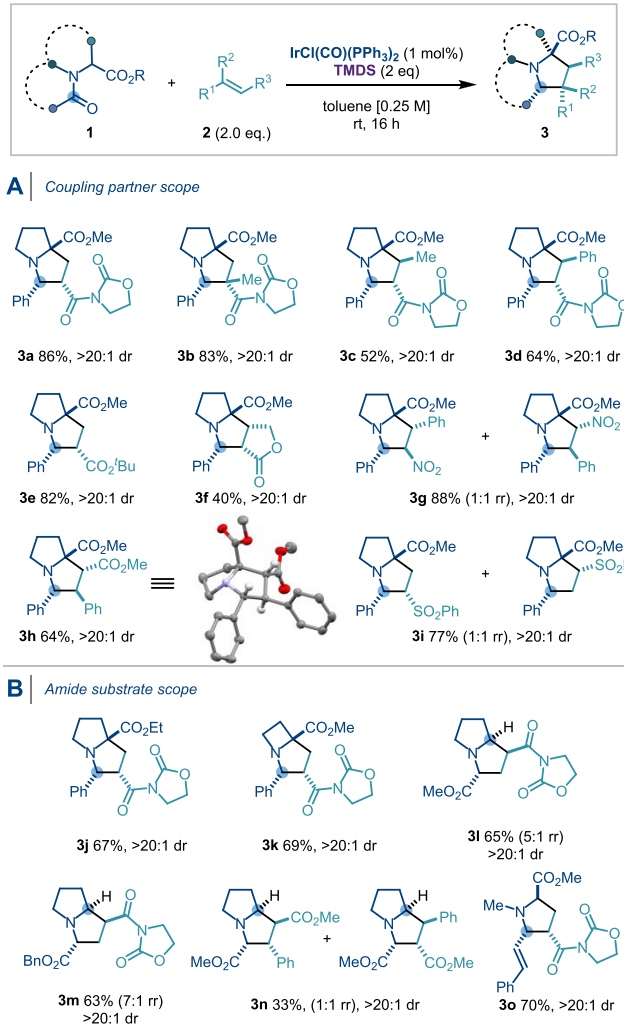

[a]Standard conditions: **1** (0.25 mmol), **2** (0.5 mmol), $IrCl(CO)(PPh_3)_2$ (1 mol %), TMDS (0.5 mmol), toluene (1 mL), rt, 16 h; yields of purified product following flash column chromatography. CCDC number for **3h**: 2056518. dr: diastereomeric ratio. rr: regioisomeric ratio.

This also demonstrated that the methodology was not limited to the reduction of reactive benzoyl amides, therefore increasing the diversity of scaffolds made accessible. A range of 2-carboxy-substituted pyrrolizidine was thus obtained with a 4-carbonyl (**3l, 3m**) or 3-aryl 4-carbomethoxy (**3n**) substitution pattern. Cinnamoyl amide **1o** also gave rise to the 4-alkenyl trisubstituted pyrrolidine **3o** in good yield.

Having established that amides and lactams possessing a β-ester appendage on the nitrogen atom were excellent precursors to stabilized azomethine ylides, we next turned our attention to unstabilized 1,3-dipole generation. Using *N*-(trimethylsilyl)methyl amides as substrates, and following standard conditions for Vaska's complex-catalyzed hydrosilylation, with substoichiometric amounts of TMSCl as an additive to trigger the desilylation, we were pleased to observe [3 + 2] dipolar cycloaddition of unstabilized azomethine ylides taking place. This approach is complementary to the one described above, as the resulting pyrrolidine ring of the cycloadduct bears no substituent *a* to the nitrogen atom. As shown in Scheme 4, the reaction was found to be tolerant of a good range of aryl and heteroaryl amides, although alkyl amides remained difficult substrates due to the rapid formation of reactive enamine species. Pleasingly, diastereocontrol was improved by increasing the steric demand of the substituent on the amide nitrogen (R) from methyl (**5a**) to benzyl (**5b**). Aryl amides containing both electron-donating (methoxy, methyl) and electron-withdrawing (halides, nitro, and nitriles) groups afforded the corresponding pyrrolidines with good to excellent diastereoselectivity (**5c**−**5k**). Heteroaromatic amides also underwent cycloaddition smoothly (**5l**, **5m**). Alkyl amide substrates gave a complex mixture, indicating a lack of regio- and diastereocontrol. Several other dipolarophiles could also be used, leading to products derived from *tert*-butyl acrylate (**5n**), dimethyl fumarate (**5o**), *N*-phenyl maleimide (**5p**), and phenyl vinyl sulfone (**5q**), although a reduced diastereoselectivity was observed (Scheme 4B). Pyrrole **5r** was obtained in a good yield using dimethyl acetylenedicarboxylate as the dipolarophile under standard conditions, followed by the oxidation of the resulting dihydropyrrolidine ring by 2,3-dichloro-5,6-dicyano-1,4-benzoquinone (DDQ). This process can provide substituted pyrroles in a one-pot sequence from inexpensive and robust tertiary amides.

Intramolecular Cyclization. To demonstrate potential applications of our methodology, a linear substrate for an intramolecular cyclization was synthesized and subjected to the reductive cycloaddition using the optimized standard conditions (Scheme 5A). Pleasingly, a remarkably chemoselective reduction of the amide carbonyl **6** was achieved, leading to the formation of the tricyclic 1-azatricyclo[3.3.0.$2^{4,6}$]decane core **7**, via the putative azomethine ylide, as a single diastereoisomer, in good yield.

Selectivity of Cycloaddition. As shown previously in Schemes 3 and 5B, the reductive [3 + 2] cycloaddition reaction showed a high regio- and diastereocontrol, according to the dipolarophile used. *N*-Enoyl oxazolidinone and *tert*-butyl acrylate gave products (**3a**, **3e**) with new C−C bond formation occurring at the carbonyl carbon atom and the α position of the alkene as a single product, whereas methyl cinnamate gave a product (**3h**) with new C−C bond formation occurring at the carbonyl carbon atom and the β position of the alkene as a single product. These results indicate that the selectivity is highly dependent on the dipolarophile, and accordingly, we turned our attention to the use of a chiral auxiliary as it can potentially give diastereo- and enantiomerically pure pyrrolidines after the removal of the oxazolidinone group. Interestingly and unexpectedly, the cycloaddition with a chiral coupling partner gave two regioisomers of the product in a 1:1 ratio and a combined 78% yield (**8a**, **8b**, Scheme 5B). These two isomers are fully separable by silica gel chromatography, and each of them is obtained essentially as a single isomer (>20:1 dr). The absolute and relative configuration of **8a** was unambiguously determined via single X-ray diffraction analysis.

MECHANISTIC INVESTIGATIONS

DFT Study. To further investigate the selectivity involved in the cycloaddition reaction, we turned to DFT calculations. Our focus was on elucidating the origin of the inversion of selectivity when methyl cinnamate was used as a coupling partner as opposed to *N*-enoyl oxazolidinone, giving, respectively, **3h** and **3d**. The regio- and diastereoselectivities

https://doi.org/10.1021/acscatal.1c01589
ACS Catal. 2021, 11, 7489−7497

Scheme 4. Substrate Scope of the [3 + 2] Cycloaddition via Unstabilized Azomethine Ylides with Regard to the Amides (A) and the Dipolarophiles (B)[a]

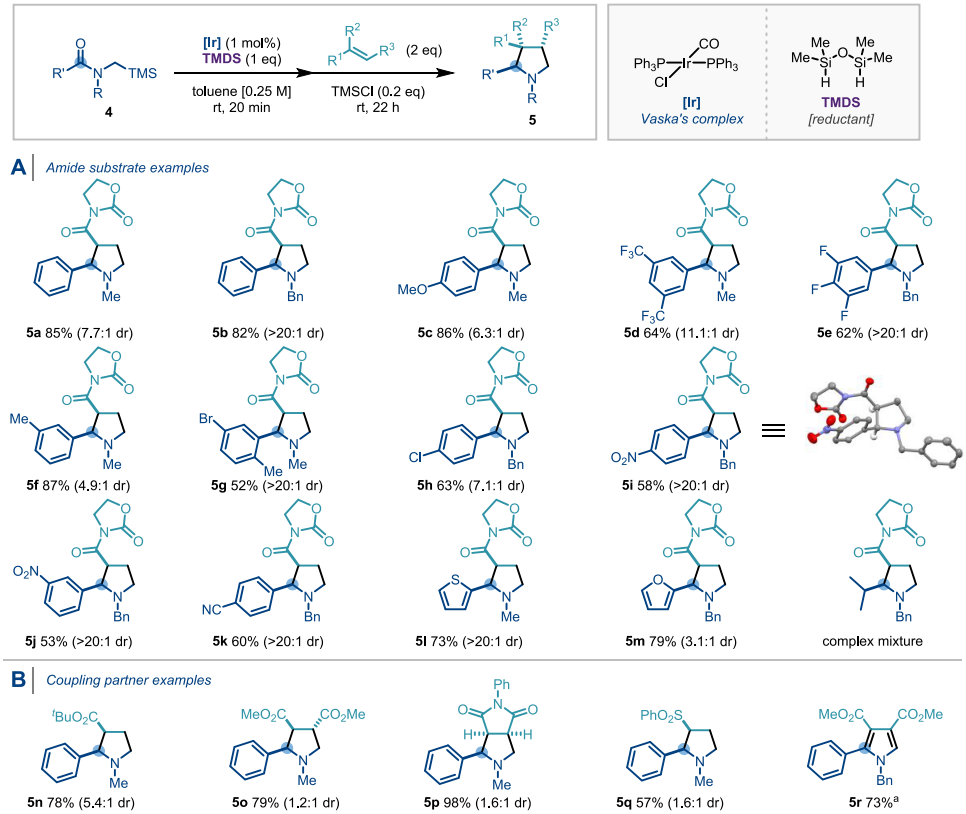

[a]Standard conditions: **4** (0.3 mmol), **2** (0.6 mmol), $IrCl(CO)(PPh_3)_2$ (1 mol %), TMDS (0.3 mmol), toluene (1 mL), rt; yields of purified product following flash column chromatography. Overall yield following the oxidation by DDQ (2.0 equiv), 80 °C, 16 h. CCDC number for **5i**: 2056517.

of the 1,3-dipolar cycloaddition involving an azomethine ylide and a dipolarophile are determined by either the strain or the interaction energies of the cycloaddition transition structures depending on the nature of the dipolarophile. The strain energy is decisive for the selectivity when the dipolarophile is methyl cinnamate, whereas the interaction energy controls for the selectivity when the dipolarophile possesses an oxazolidinone group. The origin of this unique divergent behavior depending on the structure of the dipolarophile is quantified and explained below.

The key cycloaddition transition structures between the *in situ* generated azomethine ylide[10] and methyl cinnamate or *N*-enoyl oxazolidinone are provided in Scheme 6. Among the four TSs with methyl cinnamate as the dipolarophile, the energy barrier via **TSOMe4** is the most favorable, whereas, for *N*-enoyl oxazolidinone, **TSOx2** is the most energetically favorable transition structure.[11] The origin of the kinetic preference for the regio- and diastereomer-determining cycloaddition steps was quantified using the activation strain model (ASM),[12a−d,e] also known as the distortion-interaction model.[12f,g] The ASM involves the decomposition of the electronic activation barrier ($\Delta E^{\ddagger}$) into two distinct energy terms, namely, the strain energy ($\Delta E^{\ddagger}_{strain}$) that results from the deformation of the individual reactants and the interaction energy ($\Delta E^{\ddagger}_{int}$) between the deformed reactants. These analyses have revealed that the strain energy controls the selectivity through **TSOMe4** with methyl cinnamate, while the interaction energy is decisive for the selectivity through **TSOx2** with *N*-enoyl oxazolidinone. The higher degree of asynchronicity, defined as the difference in the length of two newly forming C−C bonds in the transition structures, in **TSOMe4** leads to a less destabilizing strain energy. We recently reported the connection between asynchronicity and strain energy in the related Diels−Alder cycloaddition reaction.[13] A higher degree of asynchronicity leads to one C−C bond to form before the other and results in a smaller degree of pyramidalization (sum of angles [SoA] around a carbon atom in degrees) at the reacting carbon atoms (Scheme 7A). A good linear relationship was found between the normalized sum of angles of pyramidalization at two reacting carbon atoms (720−SoA1−SoA2 [for the dipole fragment] or 720−SoA3−SoA4 [for the dipolarophile fragment]) and the strain energies $\Delta E^{\ddagger}_{strain}$ of each fragment. Therefore, the TS that minimizes the pyramidalization of the reacting carbon atoms (SoA closer to 360°) benefits from a less destabilizing strain energy by the asynchronicity of the TS and thus a lower activation barrier if interaction energies are all similar.

On the other hand, the interaction energy was found to be operative in controlling the selectivity when the dipolarophile contains an oxazolidinone group and actually overrules the strain energy, which was decisive with the methyl cinnamate substrate, as previously discussed. The prominent role of the interaction energy on the observed reactivity trends stimulated the analysis of various contributions to the interaction using a canonical energy decomposition analysis (EDA).[14] Our canonical EDA decomposed the $\Delta E^{\ddagger}_{int}$ between the distorted reactants in the transition state into three physically meaningful energy terms: classical electrostatic interaction ($\Delta V^{\ddagger}_{elstat}$),

https://doi.org/10.1021/acscatal.1c01589
ACS Catal. 2021, 11, 7489−7497

Scheme 5. (A) Intramolecular Reductive [3 + 2] Cycloaddition. (B) Regio- and Diastereoselectivities of the Reductive [3 + 2] Cycloaddition with α,β-Unsaturated Carbonyl Compounds[a]

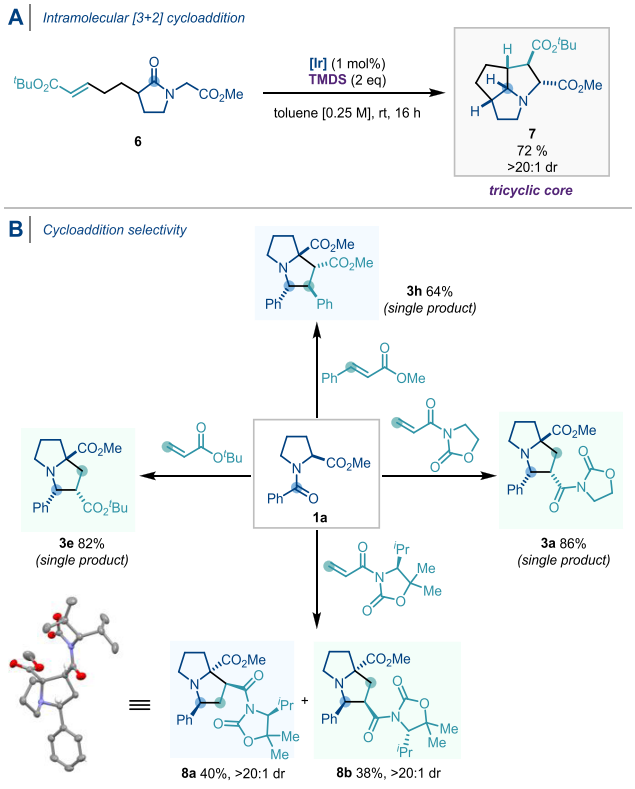

[a]CCDC for **8a**: 2056519.

steric (Pauli) repulsion ($\Delta E^{\ddagger}_{\text{Pauli}}$), which, in general, arises from the two-center four-electron repulsion between the closed-shell orbitals of both reactants, and stabilizing orbital interactions ($\Delta E^{\ddagger}_{\text{oi}}$) that account, among others, for HOMO−LUMO interactions. Analysis of EDA terms computed on the solution phase geometries in the gas phase[15] revealed that the more stabilizing orbital interactions ($\Delta E^{\ddagger}_{\text{oi}}$) and electrostatic interactions ($\Delta V^{\ddagger}_{\text{elstat}}$) for **TSOx2** set the trend in $\Delta E^{\ddagger}_{\text{int}}$. Analysis of the bonding mechanism and frontier molecular orbital (FMO) interactions revealed that the origin of the more stable $\Delta E^{\ddagger}_{\text{oi}}$ associated with **TSOx2** originates from both a smaller normal electron demand (NED) $\text{HOMO}_{\text{dipole}}$−$\text{LUMO}_{\text{alkene}}$ energy gap and the larger orbital overlap S compared to the other TSs. These combined effects result in the most stabilizing orbital interactions ($S^2/\Delta\varepsilon \times 10^3 = 9.0$) for **TSOx2** (Scheme 7B).[16] The more stable $\Delta V^{\ddagger}_{\text{elstat}}$ for **TSOx2** can be understood from analysis of the molecular electrostatic potential (MEP) maps (Scheme 7C). Here, we see that the two carbon atoms participating in the shorter newly forming C−C bond for **TSOx2** benefit from a complimentary "charge match" compared to that of **TSOx4** (the next most favorable TS). That is, the negatively charged carbon atom on the dipole and the positively charged carbon atom on the dipolarophile conveniently enter into a stabilizing electrostatic interaction, a feature that is maximized when the electron-withdrawing group on the dipole and alkene is positioned opposite of each other, such as in **TSOx2**.

CONCLUSIONS

In summary, we have developed a new, general, and highly selective reductive [3 + 2] cycloaddition reaction of amides and conjugated alkenes for structurally complex pyrrolidine synthesis. This unified strategy enabled by the use of Vaska's complex and TMDS to reductively generate a range of stabilized and unstabilized azomethine ylide species (including some inaccessible via previous nonreductive approaches), which afforded after cycloaddition a wide range of highly and diversely substituted pyrrolidines and polycyclic amine products. The reaction proceeds under mild conditions, enabling generally high diastereoselectivity and compatibility with a variety of electron-poor olefins. The use of single enantiomer or tethered dipolarophiles demonstrates applicability to the synthesis of complex and enantiopure cyclic amine architectures. The origin of high regio- and diastereoselectivities in the cycloaddition reaction was elucidated by means of density functional theory (DFT) computations. Use of the activation strain model (ASM) in conjunction with the matching canonical energy decomposition analysis (EDA) revealed that the selectivity is determined by either the strain or the interaction energies depending on the substituent on the dipolarophile. Highly asynchronous transition states are energetically preferred and go with a lower strain energy than the synchronous one, unless a highly stabilizing interaction energy between the reactants is present, in which the orbital and electrostatic interactions are decisive. Furthermore, the successful application of this method to the construction of a complex tricyclic core efficiently from a readily prepared substrate shows the potential to synthesize complex molecules possessing naturally abundant pyrrolidine scaffolds.

ASSOCIATED CONTENT

Supporting Information

The Supporting Information is available free of charge at https://pubs.acs.org/doi/10.1021/acscatal.1c01589.

Experimental procedures, NMR data, characterization, crystallographic data, and computational data (PDF)

AUTHOR INFORMATION

Corresponding Authors

Trevor A. Hamlin − *Department of Theoretical Chemistry, Amsterdam Institute of Molecular and Life Sciences (AIMMS), and Amsterdam Center for Multiscale Modeling (ACMM), Vrije Universiteit Amsterdam, 1081 HV Amsterdam, The Netherlands;* orcid.org/0000-0002-5128-1004; Email: t.a.hamlin@vu.nl

Darren J. Dixon − *Department of Chemistry, Chemistry Research Laboratory, University of Oxford, Oxford OX1 3TA, United Kingdom;* orcid.org/0000-0003-2456-5236; Email: darren.dixon@chem.ox.ac.uk

Authors

Ken Yamazaki − *Department of Chemistry, Chemistry Research Laboratory, University of Oxford, Oxford OX1 3TA, United Kingdom; Department of Theoretical Chemistry, Amsterdam Institute of Molecular and Life Sciences (AIMMS), and Amsterdam Center for Multiscale Modeling (ACMM), Vrije Universiteit Amsterdam, 1081 HV Amsterdam, The Netherlands;* orcid.org/0000-0002-2039-4321

https://doi.org/10.1021/acscatal.1c01589
ACS Catal. 2021, 11, 7489−7497

Scheme 6. Transition Structures for the 1,3-Dipolar Cycloaddition between the Azomethine Ylide and Methyl Cinnamate (A) and *N*-Enoyl Oxazolidinone (B) Computed at COSMO(Toluene)-M06-2X/TZ2P//BP86/TZ2P[a]

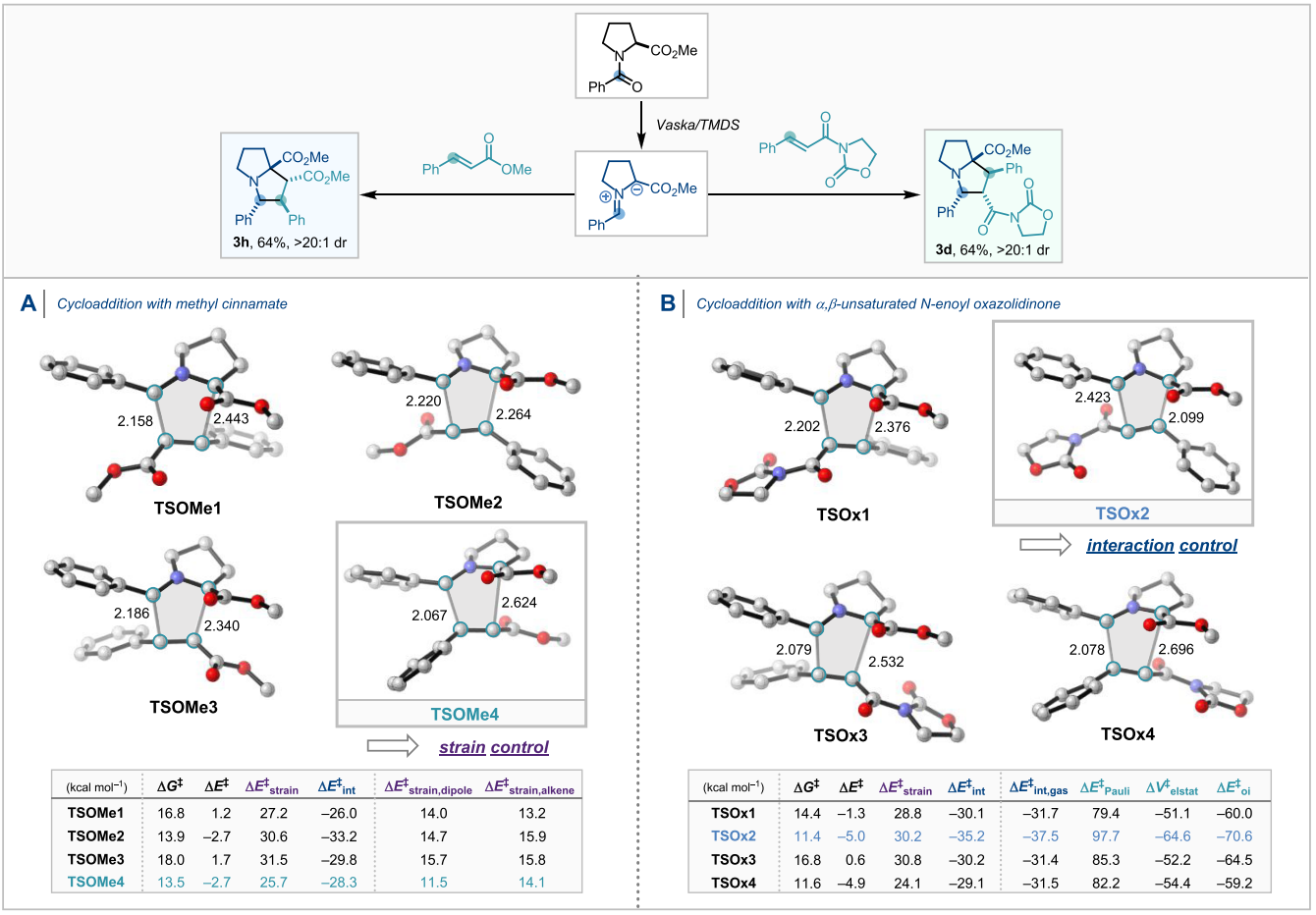

(kcal mol^{-1})	$\Delta G^{\ddagger}$	$\Delta E^{\ddagger}$	$\Delta E^{\ddagger}_{strain}$	$\Delta E^{\ddagger}_{int}$	$\Delta E^{\ddagger}_{strain,dipole}$	$\Delta E^{\ddagger}_{strain,alkene}$
TSOMe1	16.8	1.2	27.2	−26.0	14.0	13.2
TSOMe2	13.9	−2.7	30.6	−33.2	14.7	15.9
TSOMe3	18.0	1.7	31.5	−29.8	15.7	15.8
TSOMe4	13.5	−2.7	25.7	−28.3	11.5	14.1

(kcal mol^{-1})	$\Delta G^{\ddagger}$	$\Delta E^{\ddagger}$	$\Delta E^{\ddagger}_{strain}$	$\Delta E^{\ddagger}_{int}$	$\Delta E^{\ddagger}_{int,gas}$	$\Delta E^{\ddagger}_{Pauli}$	ΔV^{t}_{elstat}	$\Delta E^{\ddagger}_{oi}$
TSOx1	14.4	−1.3	28.8	−30.1	−31.7	79.4	−51.1	−60.0
TSOx2	11.4	−5.0	30.2	−35.2	−37.5	97.7	−64.6	−70.6
TSOx3	16.8	0.6	30.8	−30.2	−31.4	85.3	−52.2	−64.5
TSOx4	11.6	−4.9	24.1	−29.1	−31.5	82.2	−54.4	−59.2

[a]Energies (kcal mol^{-1}) and forming bond lengths (Å) of TS geometries are provided in the inset.

Pablo Gabriel − *Department of Chemistry, Chemistry Research Laboratory, University of Oxford, Oxford OX1 3TA, United Kingdom;* orcid.org/0000-0002-3462-5151
Graziano Di Carmine − *Department of Chemistry, Chemistry Research Laboratory, University of Oxford, Oxford OX1 3TA, United Kingdom*
Julia Pedroni − *Department of Chemistry, Chemistry Research Laboratory, University of Oxford, Oxford OX1 3TA, United Kingdom*
Mirxan Farizyan − *Department of Chemistry, Chemistry Research Laboratory, University of Oxford, Oxford OX1 3TA, United Kingdom*

Complete contact information is available at: https://pubs.acs.org/10.1021/acscatal.1c01589

Author Contributions

[§]K.Y. and P.G. contributed equally to this work.

Notes

The authors declare no competing financial interest.

■ ACKNOWLEDGMENTS

The authors thank Dr. Heyao Shi (University of Oxford) for X-ray structure determination and Dr. Amber L. Thompson and Dr. Kirsten E. Christensen (Oxford Chemical Crystallography Service) for X-ray mentoring and help. P.G. is supported by the EPSRC Centre for Doctoral Training in Synthesis for Biology and Medicine (EP/L015838/1), generously supported by AstraZeneca, Diamond Light Source, Defence Science and Technology Laboratory, Evotec, GlaxoSmithKline, Janssen, Novartis, Pfizer, Syngenta, Takeda, UCB, and Vertex. K.Y. thanks the Honjo International Scholarship Foundation for a postgraduate scholarship. T.A.H. thanks The Netherlands Organization for Scientific Research (NWO) for financial support. This work was carried out on the Dutch national e-infrastructure with the support of SURF Cooperative.

■ REFERENCES

(1) (a) Taylor, R. D.; MacCoss, M.; Lawson, A. D. G. Rings in Drugs. *J. Med. Chem.* **2014**, *24*, 5845−5859. (b) Vitaku, E.; Smith, D. T.; Njardarson, J. T. Analysis of the Structural Diversity, Substitution Patterns, and Frequency of Nitrogen Heterocycles among U.S. FDA Approved Pharmaceuticals. *J. Med. Chem.* **2014**, *57*, 10257−10274.
(2) (a) Lovering, F.; Bikker, J.; Humblet, C. Escape from Flatland: Increasing Saturation as an Approach to Improving Clinical Success. *J. Med. Chem.* **2009**, *52*, 6752−6756. (b) Lovering, F. Escape from Flatland 2: Complexity and Promiscuity. *Med. Chem. Commun.* **2013**, *4*, 515−519. (c) Aldeghi, M.; Malhotra, S.; Selwood, D. L.; Chan, A. W. E. Two-and Three-Dimensional Rings in Drugs. *Chem. Biol. Drug Des.* **2014**, *83*, 450−461.
(3) For a review on synthesis of saturated N-heterocycles, see (a) Vo, C.-V. T.; Bode, J. W. Synthesis of Saturated N-Heterocycles. *J. Org. Chem.* **2014**, *79*, 2809−2815. (b) Mitchinson, A.; Nadin, A.

Scheme 7. (A) Correlation between the Sum of Angles (SoA in degrees) and the Strain Energies of the Azomethine Ylide and the Dipolarophiles, (B) Frontier Molecular Orbital (FMO) Diagrams with Calculated Key Orbital Energy Gaps and Overlaps of the Normal Electron Demand (NED) $HOMO_{dipole}$–$LUMO_{alkene}$ Interaction, and (C) Molecular Electrostatic Potential (MEP) Map Surfaces (at 0.03 $Bohr^{-3}$) from −0.03 (Red) to 0.03 (Blue) Hartree e^{-1} of Distorted Dipole and Dipolarophile Fragments for the 1,3-Dipolar Cycloadditions between the Azomethine Ylide and the Oxazolidinone-Substituted Alkene Computed at COSMO(Toluene)-M06-2X/TZ2P//BP86/TZ2P

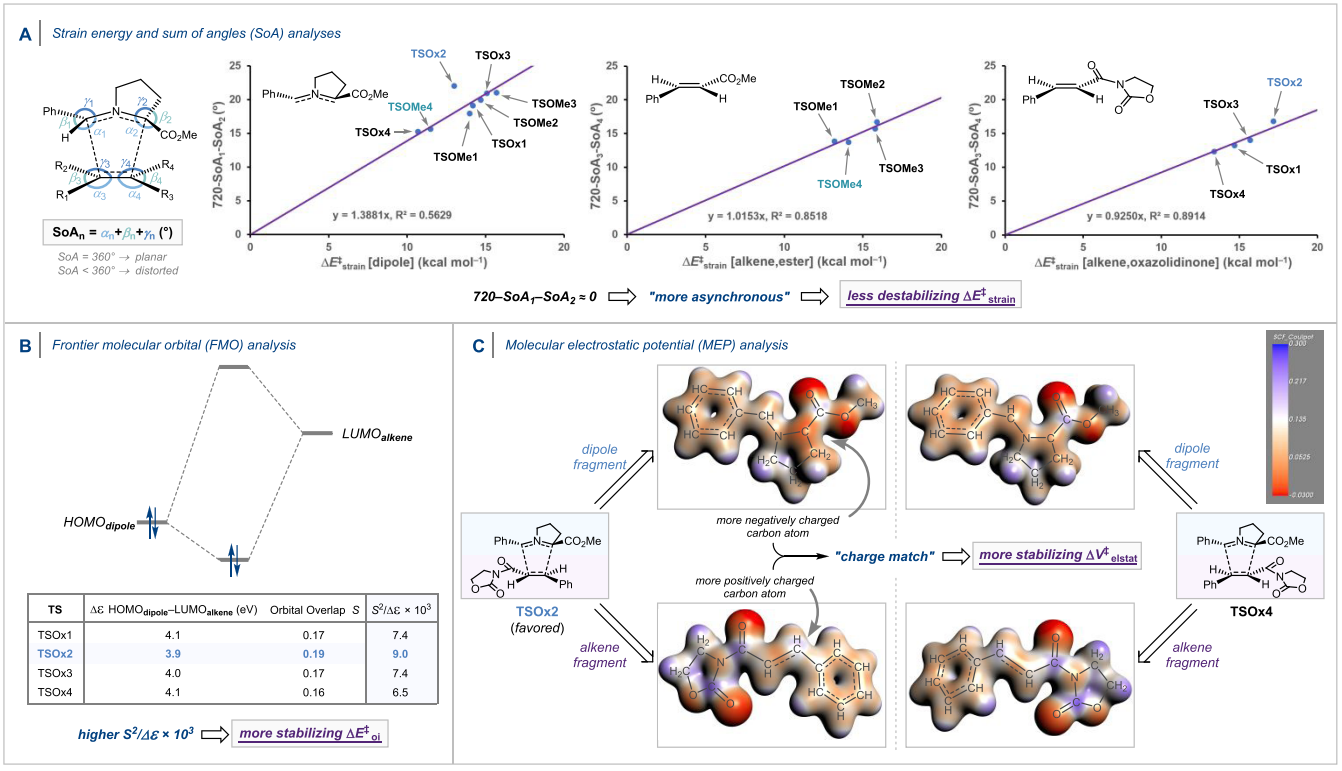

TS	Δε $HOMO_{dipole}$–$LUMO_{alkene}$ (eV)	Orbital Overlap S	$S^2/\Delta\varepsilon \times 10^3$
TSOx1	4.1	0.17	7.4
TSOx2	3.9	0.19	9.0
TSOx3	4.0	0.17	7.4
TSOx4	4.1	0.16	6.5

Saturated Nitrogen Heterocycles. *J. Chem. Soc., Perkin Trans. 1* **1999**, 2553−2581. via alkene difunctionalization, see (c) Kaur, N.; Wu, F.; Alom, N.-E.; Ariyarathna, J. P.; Saluga, S. J.; Li, W. Intermolecular Alkene Difunctionalizations for the Synthesis of Saturated Heterocycles. *Org. Biomol. Chem.* **2019**, *17*, 1643−1654.

(4) For a review on pyrrolidines and other N-heterocyclic alkaloids, see (a) O'Hagan, D. Pyrrole, Pyrrolidine, Pyridine, Piperidine, Azepine and Tropane Alkaloids. *Nat. Prod. Rep.* **1997**, *14*, 637−651. (b) O'Hagan, D. Pyrrole, Pyrrolidine, Pyridine, Piperidine and Tropane Alkaloids. *Nat. Prod. Rep.* **2000**, *17*, 435−446.

(5) For reviews on dipolar cycloaddition reactions of azomethine ylides, see (a) Nájera, C.; Sansano, J. M.; Yus, M. 1,3-Dipolar Cycloadditions of Azomethine Imines. *Org. Biomol. Chem.* **2015**, *13*, 8596−8636. (b) Ryan, J. H. 1,3-Dipolar Cycloaddition Reactions of Azomethine Ylides with Aromatic Dipolarophiles. *ARKIVOC* **2015**, *2015*, 160−183. (c) Coldham, I.; Hufton, R. Intramolecular Dipolar Cycloaddition Reactions of Azomethine Ylides. *Chem. Rev.* **2005**, *105*, 2765−2810. (d) Han, M.-Y.; Jia, J.-Y.; Wang, W. Recent Advances in Organocatalytic Asymmetric Synthesis of Polysubstituted Pyrrolidines. *Tetrahedron Lett.* **2014**, *55*, 784−794. (e) Li, J.; Ye, Y.; Zhang, Y. Cycloaddition/Annulation Strategies for the Construction of Multisubstituted Pyrrolidines and their Applications in Natural Product Synthesis. *Org. Chem. Front.* **2018**, *5*, 864−892.

(6) For methods based on aziridine ring-opening, see (a) Heine, H. W.; Peavy, R. Aziridines XI. Reaction of 1,2,3-Triphenylaziridine with Diethylacetylene Dicarboxylate and Maleic Anhydride. *Tetrahedron Lett.* **1965**, *6*, 3123−3126. (b) Padwa, A.; Hamilton, L. Reactions of Aziridines with Dimethylacetylene Dicarboxylate. *Tetrahedron Lett.* **1965**, *6*, 4363−4367. (c) Huisgen, R.; Scheer, W.; Szeimies, G.; Huber, H. 1.3-Cycloadditionen von Azomethinyliden aus Aziridincarbonestern. *Tetrahedron Lett.* **1965**, *7*, 397−404. (d) Huisgen, R.; Scheer, W.; Huber, H. Stereospecific Conversion of cis-trans Isomeric Aziridines to Open-Chain Azomethine Ylides. *J. Am. Chem. Soc.* **1967**, *89*, 1753−1755. For other [3+2] cycloaddition where the aziridine generates an alternative 1,3-zwitterionic dipoles, see (e) Ishii, K.; Shimada, Y.; Sugiyama, S.; Noji, M. Photoreactions of *β*-Aziridinylacrylonitrile. 1,3-Dipolar Cycloadditions of Photoinduced Azomethine Ylide. *J. Chem. Soc., Perkin Trans. 1* **2000**, 3022−3024. (f) Coldham, I.; Collis, A. J.; Mould, R. J.; Robinson, D. E. Pyrrolidines by 1,3-Dipolar Cycloaddition of Conjugated Azomethine Ylides. *Synthesis* **1995**, *1995*, 1147−1150. (g) Bergmeier, S. C.; Fundy, S. L.; Seth, P. P. Synthesis of Bicyclic Proline Analogs using a Formal [3 + 2] Intramolecular Aziridine-allylsilane Cycloaddition Reaction. *Tetrahedron* **1999**, *55*, 8025−8038. (h) Madhushaw, R. J.; Hu, C.-C.; Liu, R.-S. A Novel Stereocontrolled Synthesis of Cis-Fused Bicyclic Lactams via [3 + 2]-Cycloaddition of Alkynyltungsten Complexes with Tethered Aziridines. *Org. Lett.* **2002**, *4*, 4151−4153. (i) Dauban, P.; Malik, G. A Masked 1,3-Dipole Revealed from Aziridines. *Angew. Chem., Int. Ed.* **2009**, *48*, 9026−9029. For extensive reviews on methodology involving condensation of an aldehyde with a primary or secondary amine, see (j) Nájera, C.; Sansano, J. M. Azomethine Ylides in Organic Synthesis. *Curr. Org. Chem.* **2003**, *7*, 1105−1150. see also reference 5c; (k) Hashimoto, T.; Maruoka, K. Recent Advances of Catalytic Asymmetric 1,3-Dipolar Cycloadditions. *Chem. Rev.* **2015**, *115*, 5366−5412. (l) Singh, M. S.; Chowdhury, S.; Koley, S. Progress in 1,3-Dipolar Cycloadditions in the Recent Decade: An Update to Strategic Development towards the Arsenal of Organic Synthesis. *Tetrahedron* **2016**, *72*, 1603−1644. (m) Li, J.; Zhao, H.; Jiang, X.; Wang, X.; Hu, H.; Yu, L.; Zhang, Y. The Cyano Group as a Traceless Activation Group for the Intermolecular [3+2] Cycloaddition of Azomethine Ylides: A Five-Step Synthesis of (±)-Isoretronecanol. *Angew. Chem., Int. Ed.* **2015**, *54*, 6306−6310. (n) Walton, M. C.; Yang, Y.-F.; Hong, X.; Houk, K. N.; Overman, L. E. Ligand-Controlled Diastereoselective 1,3-Dipolar

https://doi.org/10.1021/acscatal.1c01589
ACS Catal. 2021, 11, 7489−7497

Cycloadditions of Azomethine Ylides with Methacrylonitrile. *Org. Lett.* **2015**, *17*, 6166−6169. (o) Lauridsen, V. H.; Ibsen, L.; Blom, J.; Jørgensen, K. A. Asymmetric Brønsted Base Catalyzed and Directed [3+2] Cycloaddition of 2-Acyl Cycloheptatrienes with Azomethine Ylides. *Chem. - Eur. J.* **2016**, *22*, 3259−3263. (p) Jia, P.; Zhang, Q.; Ou, Q.; Huang, Y. Sequential [1 + 4]- and [2 + 3]-Annulation of Prop-2-ynylsulfonium Salts: Access to Hexahydropyrrolo[3,2-b]-indoles. *Org. Lett.* **2017**, *19*, 4664−4667. (q) Corpas, J.; Ponce, A.; Adrio, J.; Carretero, J. C. Cu^{I}-Catalyzed Asymmetric [3 + 2] Cycloaddition of Azomethine Ylides with Cyclobutenones. *Org. Lett.* **2018**, *20*, 3179−3182. (r) Yang, X.-C.; Liu, J.-Y.; Liu, Z.; Hu, X.-Q.; Xu, P.-F. Quaternary Carbon Center Forming [3 + 2] Cyclization Reaction by Adjusting the Substituents of Substrates. *J. Org. Chem.* **2019**, *84*, 13871−13880. (s) Xiong, Y.; Du, Z.; Chen, H.; Yang, Z.; Tan, Q.; Zhang, C.; Zhu, L.; Lan, Y.; Zhang, M. Well-Designed Phosphine−Urea Ligand for Highly Diastereo- and Enantioselective 1,3-Dipolar Cycloaddition of Methacrylonitrile: A Combined Experimental and Theoretical Study. *J. Am. Chem. Soc.* **2019**, *141*, 961−971. (t) Padwa, A.; Gingrich, H. L.; Lim, R. Regiochemistry of Intramolecular Munchnone Cycloadditions: Preparative and Mechanistic Implications. *J. Org. Chem.* **1982**, *47*, 2447−2456. (u) Smith, R.; Livinghouse, T. An Expedient Synthetic Approach to the Physostigmine Alkaloids via Intramolecular Formamidine Ylide Cycloadditions. *J. Org. Chem.* **1983**, *48*, 1554−1555. (v) Pearson, W. H.; Clark, R. B. Formation and Cycloaddition of Nonstabilized N-Unsubstituted Azomethine Ylides from (2-Azaallyl)stannanes and (2-Azaallyl)silanes. *Tetrahedron Lett.* **1999**, *40*, 4467−4471. (w) Cattoën, X.; Solé, S.; Pradel, C.; Gornitzka, H.; Miqueu, K.; Bourissou, D.; Bertrand, G. Transient Azomethine-ylides from a Stable Amino-carbene and an Aldiminium Salt. *J. Org. Chem.* **2003**, *68*, 911−914. (x) Wolan, A.; Kowalska-Six, J. A.; Rajerison, H.; Césario, M.; Cordier, M.; Six, Y. 1,3-Dipolar Cycloadditions with Azomethine Ylide Species Generated from Aminocyclopropanes. *Tetrahedron* **2018**, *74*, 5248−5257. For examples of access to the dipole via an imidate species, see (y) Vedejs, E.; Martinez, G. R. Stereospecific Synthesis of Retronecine by Imidate Methylide Cycloaddition. *J. Am. Chem. Soc.* **1980**, *102*, 7993−7994. (z) Vedejs, E.; West, F. G. Thioimidate Methylides by the Desilylation Method: An Improved Synthesis of Pyrrolines and Pyrroles. *J. Org. Chem.* **1983**, *48*, 4773−4774. (aa) Vedejs, E.; Larsen, S.; West, F. G. Nonstabilized Imidate Ylides by the Desilylation Method: A Route to the Pyrrolizidine Alkaloids Retronecine and Indicine. *J. Org. Chem.* **1985**, *50*, 2170−2174. (bb) Cuevas, J.-C.; Patil, P.; Snieckus, V. α',α'-Disilylated Tertiary Benzamides as Dual ortho- and α'-Carbanion Synthons: Amide Peterson Olefination Routes to N-Benzoyl Enamines, Isoquinolines, and Dibenzazocines. *Tetrahedron Lett.* **1989**, *30*, 5841−5844. For a recent methodology from secondary amides via nitrilium ions, see (ac) Huang, P.-Q.; Lang, Q.-W.; Hu, X.-N. One-Pot Reductive 1,3-Dipolar Cycloaddition of Secondary Amides: A Two-Step Transformation of Primary Amides. *J. Org. Chem.* **2016**, *81*, 10227−10235. For an example of azomethine ylide generation from secondary amides, see (ad) Takahashi, Y.; Yoshii, R.; Sato, T.; Chida, N. Iridium-Catalyzed Reductive Nucleophilic Addition to Secondary Amides. *Org. Lett.* **2018**, *20*, 5705−5708. For access to nitrones 1,3-dipoles from N-hydroxy amides, see (ae) Katahara, S.; Kobayashi, S.; Fujita, K.; Matsumoto, T.; Sato, T.; Chida, N. An Iridium-Catalyzed Reductive Approach to Nitrones from N-Hydroxyamides. *J. Am. Chem. Soc.* **2016**, *138*, 5246−5249. (af) Hiraoka, S.; Matsumoto, T.; Matsuzaka, K.; Sato, T.; Chida, N. Approach to Fully Substituted Cyclic Nitrones from N-Hydroxylactam Derivatives: Development and Application to the Total Synthesis of Cylindricine C. *Angew. Chem., Int. Ed.* **2019**, *58*, 4381−4385 For a recent application in alkaloid total synthesis, see. (ag) Katahara, S.; Sugiyama, Y.; Yamane, M.; Komiya, Y.; Sato, T.; Chida, N. Five-Step Total Synthesis of (±)-Aspidospermidine by a Lactam Strategy via an Azomethine Ylide. *Org. Lett.* **2021**, *23*, 3058−3063.

(7) (a) Gregory, A. W.; Chambers, A.; Hawkins, A.; Jakubec, P.; Dixon, D. J. Iridium-Catalyzed Reductive Nitro-Mannich Cyclization. *Chem. - Eur. J.* **2015**, *21*, 111−114. (b) Tan, P. W.; Seayad, J.; Dixon, D. J. Expeditious and Divergent Total Syntheses of Aspidosperma Alkaloids Exploiting Iridium(I)-Catalyzed Generation of Reactive Enamine Intermediates. *Angew. Chem., Int. Ed.* **2016**, *55*, 13436−13440. (c) Fuentes de Arriba, A. L.; Lenci, E.; Sonawane, M.; Formery, O.; Dixon, D. J. Iridium-Catalyzed Reductive Strecker Reaction for Late-Stage Amide and Lactam Cyanation. *Angew. Chem., Int. Ed.* **2017**, *56*, 3655−3659. (d) Gammack Yamagata, A. D.; Dixon, D. J. Enantioselective Construction of the ABCDE Pentacyclic Core of the Strychnos Alkaloids. *Org. Lett.* **2017**, *19*, 1894−1897. (e) Xie, L.-G.; Dixon, D. J. Tertiary Amine Synthesis via Reductive Coupling of Amides with Grignard Reagents. *Chem. Sci.* **2017**, *8*, 7492−7497. (f) Shi, H.; Michaelides, I. N.; Darses, B.; Jakubec, P.; Nguyen, Q. N. N.; Paton, R. S.; Dixon, D. J. Total Synthesis of (−)-Himalensine A. *J. Am. Chem. Soc.* **2017**, *139*, 17755−17758. (g) Xie, L.-G.; Dixon, D. J. Iridium-Catalyzed Reductive Ugi-type Reactions of Tertiary Amides. *Nat. Commun.* **2018**, *9*, No. 2841. (h) Gabriel, P.; Gregory, A. W.; Dixon, D. J. Iridium-Catalyzed Aza-Spirocyclization of Indole-Tethered Amides: An Interrupted Pictet−Spengler Reaction. *Org. Lett.* **2019**, *21*, 6658−6662. (i) Rogova, T.; Gabriel, P.; Zavitsanou, S.; Leitch, J. A.; Duarte, F.; Dixon, D. J. Reverse Polarity Reductive Functionalization of Tertiary Amides via a Dual Iridium-Catalyzed Hydrosilylation and Single Electron Transfer Strategy. *ACS Catal.* **2020**, *10*, 11438−11447.

(8) (a) Caleffi, G. S.; Larrañaga, O.; Ferrándiz-Saperas, M.; Costa, P. R. R.; Nájera, C.; de Cózar, A.; Cossío, F. P.; Sansano, J. M. Switching Diastereoselectivity in Catalytic Enantioselective (3+2) Cycloadditions of Azomethine Ylides Promoted by Metal Salts and Privileged Segphos-Derived Ligands. *J. Org. Chem.* **2019**, *84*, 10593−10605. (b) Li, G.-Y.; Chen, J.; Yu, W.-Y.; Hong, W.; Che, C.-M. Stereoselective Synthesis of Functionalized Pyrrolidines by Ruthenium Porphyrin-Catalyzed Decomposition of α-Diazo Esters and Cascade Azomethine Ylide Formation/1,3-Dipolar Cycloaddition Reactions. *Org. Lett.* **2003**, *5*, 2153−2156. (c) Shahrestani, N.; Khosravi, H.; Jadidi, K.; Notash, B.; Naderi, S. Organocatalytic Synthesis of Enantiopure Spiro Acenaphthyl-Pyrrolizidine/Pyrrolidines: Justifying the Regioselectivity based on a Distortion/Interaction Model. *Org. Biomol. Chem.* **2019**, *17*, 7013−7024. (d) Selva, E.; Soto, J. J.; Najera, C.; Foubelo, F.; Sansano, J. M. Proline Derivatives Incorporating Hydrophobic Long-chain Derived from Natural and Synthetic Fatty Acids. *Tetrahedron* **2019**, *75*, 1378−1386. (e) Mancebo-Aracil, J.; Najera, C.; Castello, L. M.; Sansano, J. M.; Larranaga, O.; de Cozar, A.; Cossío, F. P. Regio and Diastereoselective Multicomponent 1,3-Dipolar Cycloadditions between Prolinate Hydrochlorides, Aldehydes and Dipolarophiles for the Direct Synthesis of Pyrrolizidines. *Tetrahedron* **2015**, *71*, 9645−9661.

(9) (a) Felluga, F.; Pitacco, G.; Visintin, C.; Valentin, E. Synthesis of Polysubstituted Pyrrolizidines from Proline Derivatives and Conjugated Nitroolefins. *Helv. Chim. Acta* **1997**, *80*, 1457−1472. (b) Joucla, M.; Mortier, J.; Hamelin, J. J.; Toupet, L. 1,3-Dipolar Cycloaddition Reactions of Azomethine Ylides Generated in situ through Condensation of Secondary α-Amino Esters with Benzaldehyde. *Bull. Soc. Chim. Fr.* **1988**, *1*, 143−150.

(10) Attempts to isolate or observe the dipole species by ^{1}H NMR experiments were unsuccessful owing to their extremely short lifetime.

(11) Despite a small $\Delta\Delta G^{\ddagger}$ between competing transition structures involving the methyl cinnamate or *N*-enoyloxazolidinone substrates, we note that the computations clearly indicate an energetic preference for the experimentally observed pathway.

(12) (a) van Zeist, W.-J.; Bickelhaupt, F. M. The Activation Strain Model of Chemical Reactivity. *Org. Biomol. Chem.* **2010**, *8*, 3118−3127. (b) Fernández, I.; Bickelhaupt, F. M. The Activation Strain Model and Molecular Orbital Theory: Understanding and Designing Chemical Reactions. *Chem. Soc. Rev.* **2014**, *43*, 4953−4967. (c) Wolters, L. P.; Bickelhaupt, F. M. The Activation Strain Model and Molecular Orbital Theory. *WIRES Comput. Mol. Sci.* **2015**, *5*, 324−343. (d) Bickelhaupt, F. M.; Houk, K. N. Analyzing Reaction Rates with the Distortion/Interaction-Activation Strain Model. *Angew. Chem., Int. Ed.* **2017**, *56*, 10070−10086; *Angew. Chem.* **2017**, *129*,

10204−10221. For a step-by-step protocol, see also: (e) Vermeeren, P.; van der Lubbe, S. C. C.; Fonseca Guerra, C.; Bickelhaupt, F. M.; Hamlin, T. A. Understanding Chemical Reactivity using the Activation Strain Model. *Nat. Protoc.* **2020**, *15*, 649−667. (f) Ess, D. H.; Houk, K. N. Distortion/Interaction Energy Control of 1,3-Dipolar Cycloaddition Reactivity. *J. Am. Chem. Soc.* **2007**, *129*, 10646−10647. (g) Ess, D. H.; Houk, K. N. Theory of 1,3-Dipolar Cycloadditions: Distortion/Interaction and Frontier Molecular Orbital Models. *J. Am. Chem. Soc.* **2008**, *130*, 10187−10198.

(13) Vermeeren, P.; Hamlin, T. A.; Fernández, I.; Bickelhaupt, F. M. Origin of Rate Enhancement and Asynchronicity in Iminium Catalyzed Diels−Alder Reactions. *Chem. Sci.* **2020**, *11*, 8105−8112.

(14) (a) Hamlin, T. A.; Vermeeren, P.; Fonseca Guerra, C.; Bickelhaupt, F. M. Energy Decomposition Analysis in the Context of Quantitative Molecular Orbital Theory. In *Complementary Bonding Analysis*; Grabowsky, S., Ed.; De Gruyter: Berlin, 2021; pp 199−212. (b) Bickelhaupt, F. M.; Baerends, E. J. In *Reviews in Computational Chemistry*; Lipkowitz, K. B.; Boyd, D. B., Eds.; Wiley: Hoboken, 2000; pp 1−86. (c) van Meer, R.; Gritsenko, O. V.; Baerends, E. J. Physical Meaning of Virtual Kohn−Sham Orbitals and Orbital Energies: An Ideal Basis for the Description of Molecular Excitations. *J. Chem. Theory Comput.* **2014**, *10*, 4432−4441.

(15) Hamlin, T. A.; van Beek, B.; Wolters, L. P.; Bickelhaupt, F. M. Nucleophilic Substitution in Solution: Activation Strain Analysis of Weak and Strong Solvent Effects. *Chem. - Eur. J.* **2018**, *24*, 5927−5938.

(16) Albright, T. A.; Burdett, J. K.; Wangbo, W. H. *Orbital Interactions in Chemistry*; Wiley: New York, 2013.

https://doi.org/10.1021/acscatal.1c01589
ACS Catal. 2021, 11, 7489−7497